

NONLINEAR OPTICAL PHENOMENA

PACS numbers: 42.65.Sf; 42.50.Gy
DOI: 10.1070/QE2006v036n04ABEH013146

Numerical simulation of the quasi-resonance transient double resonance regime in a scheme with the common upper level for a small inhomogeneous broadening of quantum transition lines

O.M. Parshkov

***Abstract*. The transient double resonance in the Λ-scheme is numerically investigated for short input laser pulses whose spectral widths exceed noticeably the Doppler width of quantum transitions. The case of the exact resonance is considered, when the frequencies of input pulses coincide with the central frequencies of quantum transitions, and the quasi-resonance case, when this coincidence is slightly violated. It is shown that a pulse with a lower frequency is shortened and considerably amplified during its propagation in a medium. A pulse with a higher frequency transforms to a pulse with a ridge envelope, which virtually does not decay during its propagation despite the presence of irreversible relaxation. Estimates were performed for quantum transitions in the ^{208}Pb atom.**

Keywords: *transient double resonance, inhomogeneous broadening, quasi-resonance*.

1. Introduction

Double resonance (DR) is the resonance interaction of two laser radiations with a pair of quantum transitions having a common level. Theoretical studies of pulsed DR have revealed a number of specific features of this process. Pulsed pairs were found, which were called matched pulses, for example, simultons [1 – 7] and some types of electromagnetically induced transparency (EIT) pulses [8]. In the EIT theory, pulsed pairs of the contra-intuitive sequence have been studied [8], which are close in their physical nature to pulsed pairs called adiabatons [9, 10]. A pulsed pair – a Raman soliton has been discovered, which is a combination of a bright and a dark solitons [5, 11, 12]. Pulsed pairs with considerable or even complete energy transfer from one pulse to another during their propagation in a medium were described [10, 13] and pulsed pairs in a coherently prepared medium – phaseonium [14, 15], were studied.

Analytic theories of the pulsed DR regime are usually restricted by rather rigid assumptions from the experimental point of view. For example, solutions of the simulton type in the Λ-scheme were obtained only for certain relations between the oscillator strengths of quantum transitions [1, 4] for the exact resonance. Analytic theories usually neglect the inhomogeneous broadening, although this effect was considered in the study of simultons in the Λ- and V-schemes [5, 7].

Restrictions of the analytic theory of the pulsed DR substantially complicate the experimental confirmation of its conclusions. At the same time, many experiments related, in particular, to the EIT revealed broad possibilities for applications of the pulsed DR regime [8, 16, 17]. Therefore, the use of numerical methods to find new types of pulsed pairs under conditions that are closer to real experimental situations is justified.

This paper is devoted to the numerical simulation of the DR in the Λ-scheme. The case was studied when the duration of input coherent laser pulses was considerably shorter than the irreversible relaxation time of a resonance medium and the spectra of these pulses were noticeably broader than the inhomogeneous lines of quantum transitions. When the first condition is fulfilled, the DR is usually called transient. When the second condition is fulfilled, we are dealing with the DR in the case of a small inhomogeneous broadening. The irreversible relaxation is taken into account in our paper because, as follows from calculations, the duration of one of the pulses can increase by two orders of magnitude during its propagation. The cases of the strict resonance and quasi-resonance are considered. The calculations were performed for a specific Λ-configuration of the levels of the ^{208}Pb atom, whose atomic vapour is a convenient object for experiments. The analysis performed in the paper is a continuation of studies [18] devoted to the case of a large inhomogeneous broadening of quantum transitions.

2. Formulation of the boundary-value problem

Figure 1 shows three energy levels of the ^{208}Pb atom excited by two laser beams at frequencies ω_1 (pump radiation) and ω_2 (signal radiation). The pump radiation has the left-hand circular polarisation and is quasi-resonant to the $6s^2 6p7s\,{}^3P_1^0 \leftrightarrow 6s^2 6p^2\,{}^3P_0$ transition, while the signal radiation has the right-hand circular polarisation and is quasi-resonant to the $6s^2 6p7s\,{}^3P_1^0 \leftrightarrow 6s^2 6p^2\,{}^3P_2$ transition. Let us assume that the two plane laser waves propagate together along the z axis. Then, according to the known selection

O.M. Parshkov Saratov State Technical University, ul. Politekhnicheskaya 77, 410054 Saratov, Russia; e-mail: tech@mail.saratov.ru

Received 28 November 2005
Kvantovaya Elektronika **36** (4) 333 – 338 (2006)
Translated by M.N. Sapozhnikov

rules for electric dipole transitions, the laser beams will couple together only the states $|1\rangle = |6s^2 6p^2\,{}^3P_0(0)\rangle$, $|3\rangle = |6s^2 6p7s\,{}^3P_1^0(1)\rangle$, and $|2\rangle = |6s^2 6p^2\,{}^3P_2(2)\rangle$, by forming the Λ-scheme from them (numbers in the parentheses are the quantum numbers of the projection of the total atomic momentum on the z axis). Below, we will use the notation

$$p_- = -\frac{1}{\sqrt{2}}\,(\hat{p}_x - \mathrm{i}\hat{p}_y),\ p_1 = \langle 1|p_-|3\rangle,\ p_2 = \langle 3|p_-|2\rangle,$$

where $\hat{p}_x$ and $\hat{p}_y - x$ are the x and y components of the electric dipole moment operator.

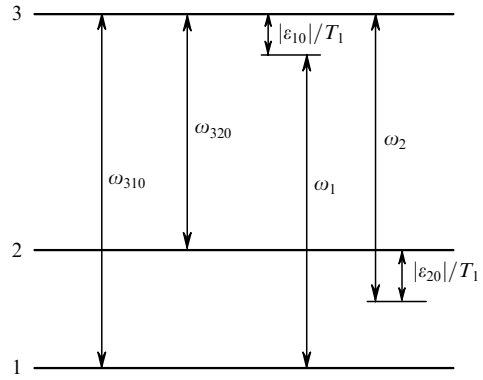

Figure 1. Scheme of quantum transitions in the ^{208}Pb atom. 1, 2, 3 are levels $6s^2 6p^2\,{}^3P_0$, $6s^2 6p^2\,{}^3P_2$, $6s^2 6p7s\,{}^3P_1^0$, respectively; ω_1 and ω_2 are the pump and signal frequencies, respectively.

Let ω_{310} and ω_{320} be the frequencies of the $|3\rangle \leftrightarrow |1\rangle$ and $|3\rangle \leftrightarrow |2\rangle$ transitions for the ^{208}Pb atom at rest in the laboratory coordinate system (Fig. 1). The frequencies ω_{31} and ω_{32} of these transitions for a moving atom differ from ω_{310} and ω_{320} due to the Doppler effect. Let us denote by T_1 the quantity inverse to the half-width (at the e^{-1} level) of the inhomogeneous $|3\rangle \leftrightarrow |1\rangle$ transition line and introduce the dimensionless detunings ε_{n0} and ε_n from the resonance:

$$\varepsilon_{n0} = T_1(\omega_{3n0} - \omega_n),\ \ \varepsilon_n = T_1(\omega_{3n} - \omega_n),\ \ n = 1, 2.$$

The quantities ε_{10} and ε_{20} (Fig. 1) characterise the degree of deviation from the resonance interaction between the laser field and a medium. The parameters ε_1 and ε_2 are expressed in terms of the velocity V_z of an atom along the z axis by the known formula for the Doppler shift and for $V_z \ll c$ are related by the expression

$$\varepsilon_2 = \varepsilon_{20} + \frac{\omega_{320}}{\omega_{310}}\,(\varepsilon_1 - \varepsilon_{10}). \tag{1}$$

The electric field strength in the Pb vapour can be written in the form

$$\boldsymbol{E} = \frac{1}{2}\,\mu_1 a_1 \boldsymbol{e}_+ \exp[\mathrm{i}(k_1 z - \omega_1 t)]$$

$$+\,\frac{1}{2}\,\mu_2 a_2 \boldsymbol{e}_+^* \exp[\mathrm{i}(k_2 z - \omega_2 t)] + \text{c.c.}, \tag{2}$$

where $a_n = a_n(z, t)$ are the complex amplitudes of the pump ($n = 1$) and signal ($n = 2$) pulses; $\mu_n = \hbar/(T_1|p_n|)$; $\boldsymbol{e}_+ = (1/\sqrt{2})(\boldsymbol{i} + \mathrm{i}\boldsymbol{j})$; and $k_n = \omega_n/c$.

Let us introduce the dimensionless independent variables

$$s = \frac{z}{x_1},\ \ w = \frac{t - z/c}{T_1},$$

where $x_1 = c\hbar/(2\pi\omega_1|p_1|^2 N T_1)$ is the distance multiplied by $\sqrt{\pi}$ at which the amplitude of weak stationary radiation at the frequency ω_{310} decreases by a factor of e due to the Doppler broadening [19]; and N is the concentration of atoms. The evolution of the fields and medium will be described by a system of Maxwell's equations for the field amplitudes a_n and amplitudes σ_{ij} $(i, j = 1, 2, 3)$ of the density matrix elements in the first approximation of the slowly varying envelope method [20, 21]

$$\frac{\partial a_1}{\partial s} = \frac{\mathrm{i}}{\sqrt{\pi}} \int_{-\infty}^{+\infty} \sigma_{31} \exp\left[-(\varepsilon_1 - \varepsilon_{10})^2\right] \mathrm{d}\varepsilon_1,$$

$$\frac{\partial a_2}{\partial s} = \frac{\mathrm{i}}{\sqrt{\pi}}\,\alpha \int_{-\infty}^{+\infty} \sigma_{32} \exp\left[-(\varepsilon_1 - \varepsilon_{10})^2\right] \mathrm{d}\varepsilon_1,$$

$$\frac{\partial \sigma_{31}}{\partial w} + \mathrm{i}\varepsilon_1 \sigma_{31} = \mathrm{i}a_1(\sigma_{11} - \sigma_{33}) + \mathrm{i}a_1\sigma_{21} - \gamma_{31}\sigma_{21},$$

$$\frac{\partial \sigma_{32}}{\partial w} + \mathrm{i}\varepsilon_2 \sigma_{32} = \mathrm{i}a_2(\sigma_{22} - \sigma_{33}) + \mathrm{i}a_1\sigma_{12} - \gamma_{32}\sigma_{32},$$

$$\frac{\partial \sigma_{21}}{\partial w} + \mathrm{i}(\varepsilon_1 - \varepsilon_2)\sigma_{21} = \frac{\mathrm{i}}{4}\,a_2^* \sigma_{31} - \frac{\mathrm{i}}{4}\,a_1 \sigma_{23}, \tag{3}$$

$$\frac{\partial \sigma_{11}}{\partial w} = \frac{1}{2}\,\mathrm{Im}(a_1 \sigma_{31}^*) + w_{31}\sigma_{33},$$

$$\frac{\partial \sigma_{22}}{\partial w} = \frac{1}{2}\,\mathrm{Im}(a_2 \sigma_{32}^*) + w_{32}\sigma_{33},$$

$$\frac{\partial \sigma_{33}}{\partial w} = -\frac{1}{2}\,\mathrm{Im}(a_1 \sigma_{31}^*) - \frac{1}{2}\,\mathrm{Im}(a_2 \sigma_{32}^*)$$

$$-(w_{31} + w_{32} + \gamma_3)\sigma_{33}$$

with parameters ε_1 and ε_2 related by expression (1). Here, $\alpha = \omega_{320}|p_2|^2/(\omega_{310}|p_1|^2)$ is the ratio of the oscillator strengths for the $2 \leftrightarrow 3$ and $1 \leftrightarrow 3$ transitions. The state $|3\rangle$ spontaneously decays to different states of the $6s^2 6p^2\,{}^3P_2$ and $6s^2 6p^2\,{}^3P_0$ levels, and the $6s^2 6p^2\,{}^3P_1$ level [22] not shown in Fig. 1. For this reason, the relaxation terms are introduced into Eqns (3), which contain the probabilities w_{31} and w_{32} of the spontaneous $|3\rangle \to |1\rangle$ and $|3\rangle \to |2\rangle$ transitions, the decay probabilities γ_{31} and γ_{32} for the amplitudes σ_{31} and σ_{32}, and the probability γ_3 of spontaneous decay of the state $|3\rangle$ to different states of the $6s^2 6p^2\,{}^3P_1$ level (all the probabilities are measured in units of T_1^{-1}). The calculations were performed for the concentration $N = 9.6 \times 10^{12}$ cm^{-3} of the saturated ^{208}Pb vapour at $T = 900$ K [23]. Then, the normalisation constants for time and distance take the values $T_1 = 1.7 \times 10^{-10}$ s and $x_1 = 0.12$ cm. The oscillator strengths for the $6s^2 6p^2\,{}^3P_0 \to 6s^2 6p7s\,{}^3P_1^0$ and $6s^2 6p^2\,{}^3P_2 \to 6s^2 6p7s\,{}^3P_1^0$ transitions

are 0.197 and 0.142, respectively [22]. By using these data and operation rules for angular momentum operators [24], we can easily obtain $|p_1| = 2.0 \times 10^{-18}$ cgs units, $|p_2| = 3.48 \times 10^{-18}$ cgs units and find other dimensionless parameters of quantum transitions: $\omega_{320}/\omega_{310} = 0.7$, $\alpha = 2.1$, $\gamma_{31} = \gamma_{32} = 1.5 \times 10^{-2}$, $w_{31} = 9.3 \times 10^{-3}$, $w_{32} = 9.5 \times 10^{-3}$, and $\gamma_3 = 1.1 \times 10^{-2}$.

System (3) was supplemented with the initial conditions describing the unperturbed medium in which all the atoms are in the ground state $|1\rangle$: $\sigma_{ij}(s, w = 0)$ and all other $\sigma_{11}(s, w = 0) = 1$ are zero. The boundary conditions for the fields on the input surface of the vapour volume $s = 0$ were written in the form

$$a_n(s = 0, w) = a_{n0} \operatorname{sech} \frac{w - 3}{0.2}, \quad n = 1, 2, \tag{4}$$

where a_{n0} is the maximum value of the envelope a_n. The duration τ of pulses (4) [full width at half-maximum (FWHM)] in units of T_1 was 0.53, which is considerably shorter than the relaxation times γ_{31}^{-1}, γ_{32}^{-1}, w_{31}^{-1}, w_{32}^{-1}, γ_3^{-1} (transient DR regime). The spectral width (FWHM) of each pulse (4) was five times greater than that of the inhomogeneous pump line (DR at a small inhomogeneous broadening of quantum transitions).

The boundary-value problem for system (3) was solved numerically by using the program based on the predictor–corrector scheme with the calculation accuracy control according to the Runge rule [25]. This program provides the reliable simulation of the transient DR [18] and processes related to self-induced transparency (SIT) [26].

3. Method for representing calculation results

The results of calculations are represented by plots of the real envelopes $E_n(w) = |a_n(s, w)|$ and phase shifts $\phi_n(w) = \arg a_n(s, w)$ for fixed values of s [$-\pi < \phi_n(w) \leqslant \pi$]. Areas under the plots of the real and imaginary parts of the complex envelope $a_1(s, w)$ for fixed s are denoted by $\Theta_1'(s)$ and $\Theta_1''(s)$, respectively. The functions $E_{m1}(s) = \max E_1(w)$ and $E_{m2}(s) = (\mu_1/\mu_2) \max E_2(w)$ are the maximal values of real envelopes of pulses measured in units of μ_1^{-1} for fixed s. The pulse FWHM in units of T_1 is denoted by τ.

As the frequency characteristics of the pump ($n = 1$) and signal ($n = 2$) pulses, the quantities $\tilde{\varepsilon}_{n0} = T_1(\omega_{3n0} - \tilde{\omega}_n)$ are used, where $\tilde{\omega}_n$ is the instant frequency of the pulse. It can be easily shown that $\tilde{\varepsilon}_{n0} = \varepsilon_{n0} + \partial\phi_n/\partial w$. The spectral density $\Omega_n(\Delta)$ of the pulse, where $\Delta = T_1(\omega_n - \omega')$, is defined as the modulus of the Fourier transform of the function $(2/\mu_n T_1)\boldsymbol{e}\boldsymbol{E}_n$ at the frequency ω'. Here, $\boldsymbol{E}_n$ is the total electric field strength of the pulse, $\boldsymbol{e} = \boldsymbol{e}_+$ for $n = 1$ and $\boldsymbol{e} = \boldsymbol{e}_+^*$ for $n = 2$.

4. Results of calculations

1. Let us set $a_{10} = 8$ and $a_{20} = 0.3$ in (4) and assume that the condition of the exact resonance $\varepsilon_{10} = \varepsilon_{20} = 0$ is fulfilled. (The FWHM of both pulses is 90 ps, the peak intensity is 75 and 35 kW cm^{-2}, respectively.) In this case, $\Theta_1'(0)$ is equal to 1.6π and represents the area of the input pump pulse in terms of the SIT theory [27]. According to [27], in the absence of signal radiation, a single 2π pulse should be formed in the pump channel.

The plots of real envelopes $E_1(w)$ and $E_2(w)$ of the pump and signal at the distance $s = 60$ are presented in Fig. 2. Figure 3 shows the dependences $E_{mn}(s)$ and $\Theta_1'(s)$. Note that the pump pulse in Fig. 2a contains many spikes and its total duration is much greater than that of the input pump pulse. The signal pulse in Fig. 2b consists of two parts: the leading pulse (*1*) and its 'tail' (*2*). The peak intensity of the leading pulse is more than 50 times higher (i.e., its peak energy density flux is approximately 2500 times higher) than that of the input signal pulse and its duration is smaller by a factor of 1.6.

Our calculations showed that in this case both amplitudes a_1 and a_2 are real, i.e., the interacting pulses have no phase modulation. In this case, at points in Fig. 2a where $E_1(w)$ vanishes, the phase shift $\phi_1(w)$ experiences a jump equal to π, preserving a constant value between these points, which is equal to zero or π. This means that the pump pulse

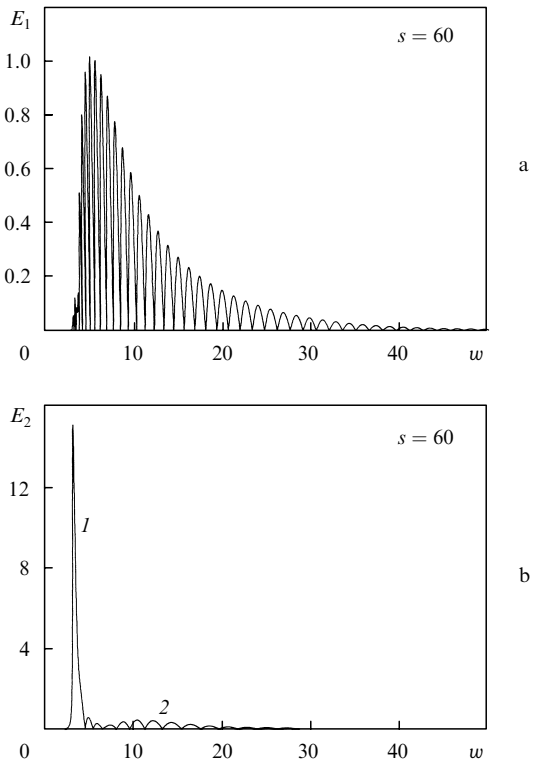

Figure 2. Envelopes of the pump E_1 (a) and signal E_2 (b) pulses for $s = 60$ in the case of the exact resonance.

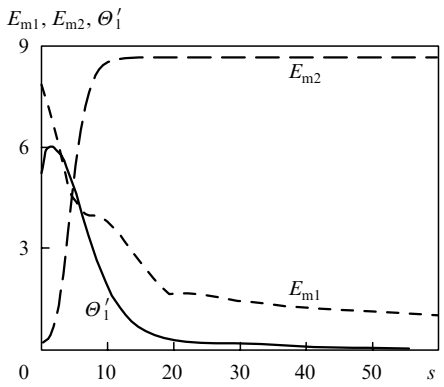

Figure 3. Maximum value of the envelope of the pump and signal pulses E_{m1} and E_{m2}, respectively, and the area Θ_1' under the envelope a_1 as functions of s in the case of the exact resonance.

is similar to a weak strictly resonance 0π pulse [28] described in the SIT theory. This is confirmed by the curve Θ_1' in Fig. 3, which demonstrates that the area Θ_1' under the plot of the envelope a_1 decreases with increasing s and becomes virtually zero for $s = 60$. This curve also shows that the pump pulse can be treated as the 0π pulse already for $s > 20$. The curve E_{m1} in Fig. 3 shows that the pump has a noticeable intensity at large s and very weakly decreases with distance. Thus, for $s = 20 - 60$, the value of E_{m1} decreases approximately by a factor of 1.6, whereas the field strength of a weak stationary resonance radiation at this distance should decrease due to the inhomogeneous broadening [19] more than by 10^{30} times. The curves E_{m2} and Θ_1' in Fig. 3 and a detailed analysis of the envelopes $E_2(w)$ show that the efficient energy transfer from the pump to signal and variations in the parameters of the latter cease after the transformation of the pump pulse to the 0π pulse (in our case, for $s > 20$).

The spectral densities of the pump and signal pulses for $s = 60$ are presented in Fig. 4. These dependences will be discussed below.

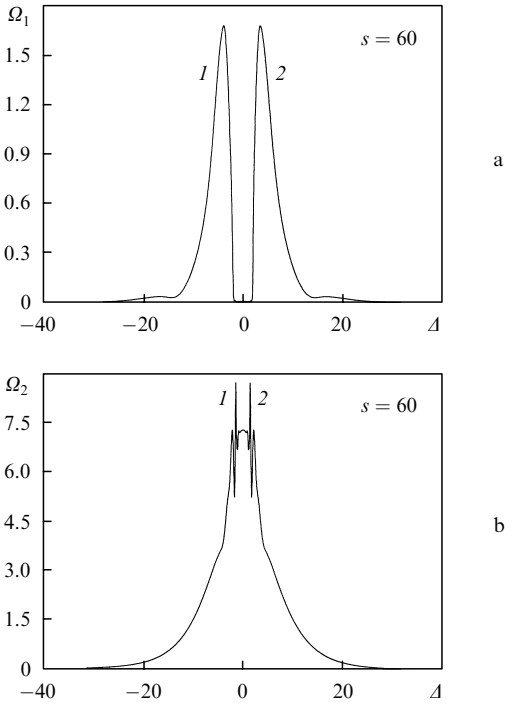

Figure 4. Spectra of the pump (a) and signal (b) pulses for $s = 60$ in the case of the exact resonance.

2. Let us set $\varepsilon_{10} = \varepsilon_{20} = 1$, by preserving the other conditions of the previous calculation invariable. In this quasi-resonance case, the envelopes a_n prove to be complex and the phase modulation of both radiations appears.

Figure 5 shows the dependences $E_{mn}(s)$, $\Theta_1'(s)$, and $\Theta_1''(s)$. The curves in Fig. 5a demonstrate that the energy transfer from the pump to signal pulse occurs efficiently only at the distance $s < 25$ from the input surface. Then, the pump pulse of a noticeable intensity very weakly decays with increasing s, similarly to the 0π pump pulse in the previous calculation.

Figure 6 presents the real envelope E_1 of the pump pulse for $s = 300$. The ridge structure of this envelope differs from

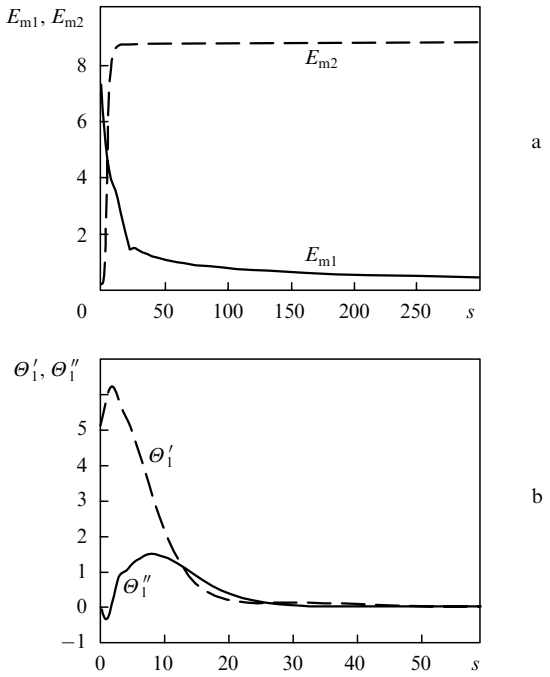

Figure 5. Dependences of the maximum value of the envelope of the pump and signal pulses E_{m1} and E_{m2} (a) and areas Θ_1' and Θ_1'' under the real and imaginary parts of the envelope a_1 (b) on s for $\varepsilon_{10} = \varepsilon_{20} = 1$.

that of the 0π pulse in Fig. 2a in that the bases of the peaks are not located in general on the abscissa axis. The pulse is phase-modulated [a fragment of the plot $\phi_1(w)$ is presented in Fig. 7] and can be treated as the 0π pulse in the quasi-resonance case. This consideration is substantiated in Fig. 5b, which shows that both areas Θ_1' and Θ_1'' vanish at large s. Recall that for a strictly resonance 0π pulse described in the SIT theory, $\Theta_1' = 0$ and $\Theta_1'' = 0$, the second equality being provided by the condition $\mathrm{Im}\, a_1 = 0$ for all values of s and w. In the case under study, $\mathrm{Im}\, a_1$ differs from zero. Note that the total duration of the pulse shown in Fig. 6 is approximately two orders of magnitude greater than that of the input pump pulse and is approximately equal to the transverse relaxation time γ_{31}^{-1} for the 1–3 transition.

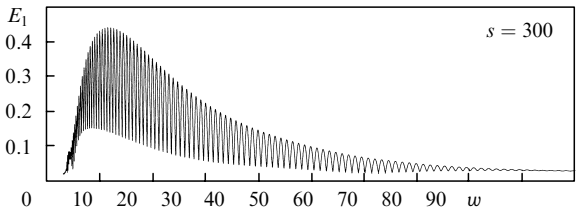

Figure 6. Envelope E_1 of the pump pulse for $s = 300$ and $\varepsilon_{10} = \varepsilon_{20} = 1$.

The plots of the real envelope $E_2(w)$ for $s > 25$, when the signal gain is already saturated, virtually coincide with the plots $E_2(w)$ in the case of the exact resonance for $s > 20$ (see, for example, Fig. 2b) and therefore are not presented here. However, the signal radiation is now phase-modulated, and for $s = 300$ the frequency $\tilde{\omega}_2$ is shifted with respect to the frequency ω_2 so that $\tilde{\varepsilon}_{20} = 0.92$ ($\tilde{\varepsilon}_{20} = \varepsilon_{20} = 1$ on the input surface). The spectral densities of pump and signal pulses for $s = 300$ are presented in Fig. 8.

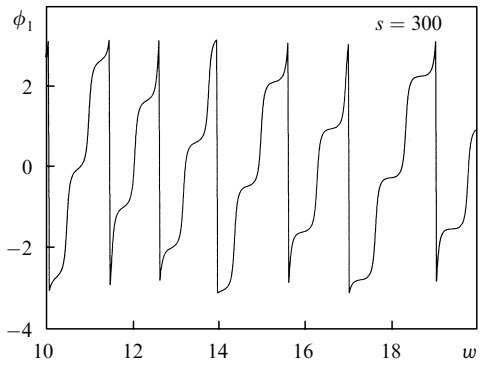

Figure 7. Fragment of the plot of the phase shift ϕ_1 of the pump pulse for $s = 300$ and $\varepsilon_{10} = \varepsilon_{20} = 1$.

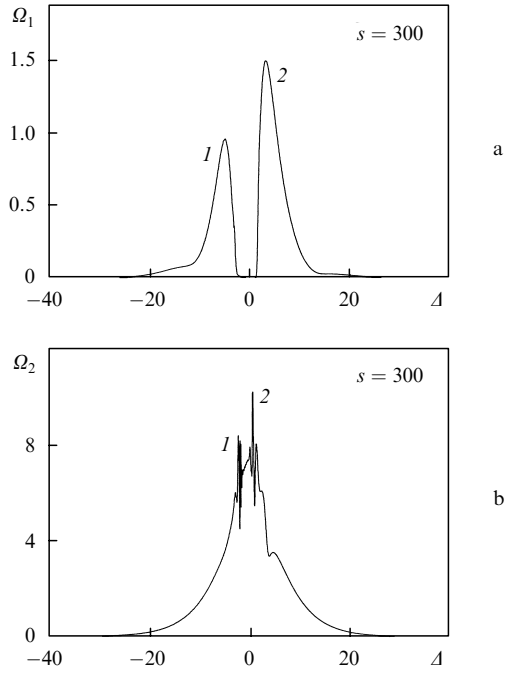

Figure 8. Spectra of the pump (a) and signal (b) pulses for $s = 300$ and $\varepsilon_{10} = \varepsilon_{20} = 1$.

3. Let us set now $\varepsilon_{10} = 1$ and $\varepsilon_{20} = -1$, preserving all the other parameters invariable. The numerical analysis showed that the plots of envelopes $E_1(w)$ and $E_2(w)$ and of functions $E_{mn}(s)$, $\Theta_1'(s)$, and $\Theta_1''(s)$ virtually coincide with the corresponding plots calculated above. The reason is as follows. Near the input surface ($s < 8$), when the signal pulse is still weak, its instant frequency $\tilde{\omega}_2$ changes so that the equality $\tilde{\varepsilon}_{20} = 1$ begins to be fulfilled. This value of $\tilde{\varepsilon}_{20}$ coincides with the value of ε_{20} specified in the previous calculation. Therefore, the instant frequencies of signal pulses become identical already near the input surface; the further evolution of the pulses also occurs identically. Such a signal-frequency locking in the case of a weak signal radiation in the absence of the inhomogeneous broadening was discovered in theoretical paper [29].

4. The appearance of ridge pulses in the pump channel can be simply explained from the physical point of view. The spectral density Ω_1 of the input pulse has the shape of a symmetric bell. The spectral harmonics resonant with the inhomogeneously broadened transition decay during their propagation and transfer their energy to the signal radiation and the resonance medium. As a result, the pump spectrum for large s consists of two spectral lines of a finite width. In the case of the exact resonance, the frequencies of the absorbed harmonics are located symmetrically with respect to the central frequency of the spectrum of the input pump pulse, while in the quasi-resonance case, they are shifted with respect to this frequency. Therefore, for $\varepsilon_{10} = 0$, the spectral lines are identical (Fig. 4a), whereas for $\varepsilon_{10} \neq 0$ their peak intensities are different (Fig. 8a). Let us denote the areas of spectral curves (*1*) and (*2*) by b_1 and b_2 in Figs 4a and 8a and approximate the spectral densities shown in these figures by two infinitely narrow lines:

$$\Omega_1(\Delta) = b_1\delta(\Delta - \Delta_1) + b_2\delta(\Delta - \Delta_2), \tag{5}$$

where Δ_1 and Δ_2 are the positions of the maxima of spectral peaks (*1*) and (*2*). It can be easily shown that spectrum (5) corresponds to the sinusoidal oscillation with the frequency ω_1 and variable amplitude whose dependence of w is described by the function

$$E_1(w) = \left\{b_1^2 + b_2^2 + 2b_1b_2\cos[\xi(\Delta_2) - \xi(\Delta_1) - (\Delta_2 - \Delta_1)w]\right\}^{1/2}, \tag{6}$$

where $\xi(\Delta_1)$ and $\xi(\Delta_2)$ are the phases of harmonics at the frequencies Δ_1 and Δ_2, whose values are now inessential. Amplitude (6) has the period $\tau_1 = 2\pi/(\Delta_2 - \Delta_1)$ and specifies the modulation depth $\eta = 2l/(1 + l)$, where $l = b_1/b_2$, by assuming that $b_1 \leqslant b_2$. Here, $\eta = (E_{max} - E_{min})/E_{max}$, where E_{max} and E_{min} are the maximum and minimum values of amplitude (6). We can assume approximately that $l \approx \Omega_{1\,max}/\Omega_{2\,max}$, where $\Omega_{1\,max}$ and $\Omega_{2\,max}$ are the peak intensities of spectral lines (*1*) and (*2*) in Figs 4a and 8a.

We have from Fig. 8a that $\Delta_2 - \Delta_1 = 8.2$ and $l = 0.6$, so that $\tau_1 = 0.8$ and $\eta = 0.7$. The values of τ_1 and η in the region of the most intense spike in Fig. 6 are 0.6 and 0.8, respectively, which is close to the values presented above. It follows from Fig. 4a that $\Delta_2 - \Delta_1 = 7.2$, $l = 1$. Then, $\tau_1 = 0.8$ and $\eta = 1$. This value of τ_1 also well agree with the characteristic distance between spikes in Fig. 2a, while the equality $\eta = 1$, meaning that $E_{min} = 0$, is confirmed by this figure. These coincidences suggest that the ridge structure of the pump pulse envelope is the result of its specific spectrum.

For peaks (*1*) and (*2*) in Figs 4b and 8b, we have $\Delta_2 - \Delta_1 = 2.8$, which corresponds to the repetition period of the envelope spikes equal to 2.2. This value is in good agreement with the characteristic distance between the spikes of the tail of the signal pulse in Fig. 2b, which means that spikes (*1*) and (*2*) belong to the spectrum of this 'tail'. Note that the presence of spectral spikes corresponding to the tails of intense pulses in the case of a small inhomogeneous broadening of spectral lines was theoretically discovered in the study of the formation of 2π pulses [30].

5. Consider the case of a more intense input pump pulse, by setting $a_{10} = 16$ in (4). We assume that $\varepsilon_{10} = \varepsilon_{20} = 2$ and other calculation parameters are the same as in paragraphs 1–3 of this section. In this case, $\Theta_1'(0) = 3.2\pi$, and in the absence of signal radiation, the formation of two 2π pulses at the pump frequency is expected [27]. Figure 9 presents the

plots of envelopes $E_1(w)$ and $E_2(w)$ for $s = 800$. (The long oscillating 'tail' of the envelope located in the region $w = 12-100$ lies outside Fig. 9.) One can see that now the main part of the ridge pulse is substantially shorter than the ridge pulse calculated in paragraphs 2, 3. The peak value of the signal pulse in Fig. 9b is more than three times greater than that calculated in paragraphs 1–3, whereas its duration $\tau = 0.13$ is three times shorter than that of the signal pulse obtained in these calculations.

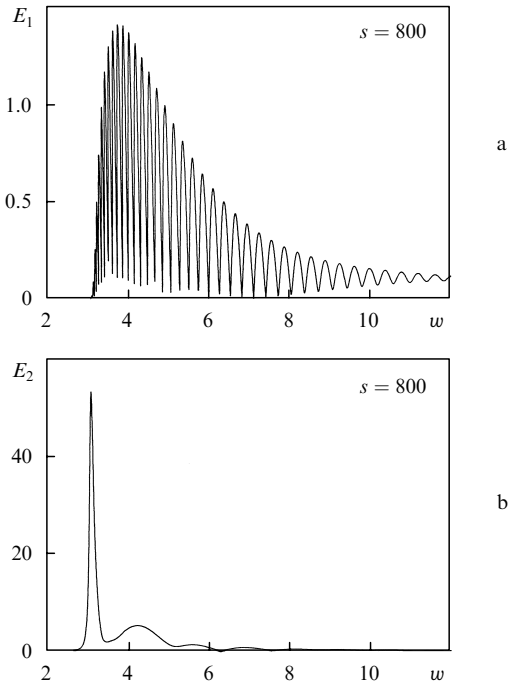

Figure 9. Envelope of the pump E_1 (a) and signal E_2 (b) pulses for $s = 800$ and the doubled amplitude of the input pump pulse in the case $\varepsilon_{10} = \varepsilon_{20} = 2$.

5. Conclusions

The transient DR has been numerically simulated in the case of a small Doppler broadening of spectral lines. It has been found that the duration of the signal pulse decreases during its propagation in a resonance medium, while its peak intensity considerably increases. The parameters of the signal pulse cease to change when a ridge pulse is formed in the pump channel. A particular case of this pulse is a weak exactly resonance 0π pulse described in the SIT theory. (The SIT theory also describes high-power 0π pulses – breathers [31].) Because the spectrum of the ridge pulse does not contain harmonics at the resonance-transition frequency, this pulse, despite its rather long duration that is close to the irreversible relaxation time, extremely weakly decays during its propagation. The appearance of the ridge pulse restricts the energy transfer from the pump to signal pulse. On the other hand, the ability of this pulse to propagate virtually without dissipation in a resonance medium makes it an interesting object for theoretical and experimental studies.

The choice of the energy levels of the ^{208}Pb isotope for the study in this paper is explained by the following considerations. The energy spectrum of this Pb isotope has no the hyperfine structure and thus is sufficiently adequate to the model proposed in the paper. In addition, the transitions in the ^{208}Pb isotope studied in the paper have been used in EIT experiments [32]. The conditions of these experiments are close to those required for the observation of effects described in our paper. However, the input pulses corresponding to our model should be shorter and more intense than those considered in [32].

Acknowledgements. The author thank A.E. Dmitriev for useful discussions of the paper.

References

1. Konopnicki M.J., Eberly J.H. *Phys. Rev. A*, **24**, 2567 (1981).
2. Stroud C.R. Jr., Cardimona D.A. *Opt. Commun.*, **37**, 221 (1981).
3. Maimistov A.I. *Kvantovaya Elektron.*, **11**, 567 (1984) [*Sov. J. Quantum Electron.*, **14**, 385 (1984)].
4. Andreev A.V. *Zh. Eksp. Teor. Fiz.*, **113**, 747 (1998).
5. Rahman A., Eberly J.H. *Phys. Rev. A*, **58**, R805 (1998).
6. Rahman A. *Phys. Rev. A*, **60**, 4187 (1999).
7. Sazonov S.V. *Izv. Ross. Akad. Nauk, Ser. Fiz.*, **66**, 353 (2002).
8. Harris S.E. *Phys. Today*, **50**, 36 (1997).
9. Grob R., Hioe F.T., Eberly J.H. *Phys. Rev. Lett.*, **73**, 3183 (1994).
10. Arkhipkin V.G., Timofeev I.V. *Kvantovaya Elektron.*, **30**, 180 (2000) [*Quantum Electron.*, **30**, 180 (2000)].
11. Ackerhalt J.R., Milonni P.W. *Phys. Rev. A*, **33**, 3185 (1986).
12. Eberly J.H. *Quant. Semiclass. Opt.*, **7**, 373 (1995).
13. Bol'shov L.A., Elkin N.N., Likhanskii V.V., Persiantsev M.I. *Zh. Eksp. Teor. Fiz.*, **88**, 47 (1985); Bol'shov L.A., Likhanskii V.V. *Kvantovaya Elektron.*, **12**, 1339 (1985) [*Sov. J. Quantum Electron.*, **15**, 889 (1985)].
14. Scully M.O. *Phys. Rev. Lett.*, **67**, 1855 (1991).
15. Eberly J.H., Rahman A. *Phys. Rev. Lett.*, **76**, 3687 (1996).
16. Marangos J.P. *J. Mod. Opt.*, **45**, 471 (1998).
17. Arkhipkin V.G., Timofeev I.V. *Pis'ma Zh. Eksp. Teor. Fiz.*, **76**, 74 (2002).
18. Dmitriev A.E., Parshkov O.M. *Kvantovaya Elektron.*, **35**, 749 (2005) [*Quantum Electron.*, **35**, 749 (2005)].
19. Akulin V.M., Karlov N.V. *Intensivnye rezonansnye vzaimodeistviya v kvantovoi elektronike* (Intense Resonance Interactions in Quantum Electronics) (Moscow: Nauka, 1987).
20. Akhmanov S.A., Khokhlov R.V. *Problemy nelineinoi optiki: Elektromagnitnye volny v nelineinykh dispergiruyushchikh sredakh, 1962-1963* (Problems of Nonlinear Optics: Electromagnetic Waves in Nonlinear Dispersive Media, 1962-1963) (Moscow: Izd. Akad. Nauk SSSR, 1965).
21. Butylkin V.S., Kaplan A.E., Khronopulo Yu.G., Yakubovich E.I. *Rezonansnye vzaiomodeistviys sveta s veshchestvom* (Resonance Interactions of Light with Matter) (Moscow: Nauka, 1977).
22. DeZafra R.L., Marshall A. *Phys. Rev.*, **170**, 28 (1968).
23. Grigor'ev I.S., Meilkhov E.Z. (Eds) *Fizicheskie velichiny. Spravochnik* (Handbook of Physical Quantities) (Moscow: Energoizdat, 1991).
24. Sobelman I.I. *Introduction to the Theory of Atmomic Spectra* (New York: Pergamon Press, 1972; Moscow: Nauka, 1977).
25. Bakhvalov N.S., Zhidkov N.P., Kobel'kov G.M. *Chislennye metody* (Numerical Methods) (Moscow: Fizmatlit, 2002).
26. Vershinin A.L., Dmitriev A.E., Parshkov A.M. *Kvantovaya Elektron.*, **33**, 993 (2003) [*Quantum Electron.*, **33**, 993 (2003).
27. McCall S.L., Hahn E.L. *Phys. Rev.*, **183**, 457 (1969).
28. Crisp M.D. *Phys. Rev. A*, **1**, 1604 (1970).
29. Dmiriev A.E., Parshkov O.M. *Kvantovaya Elektron.*, **13**, 712 (1986) [*Sov. J. Quantum Electron.*, **16**, 464 (1986)].
30. Schupper N., Friedmann H., Matusovsky M., Rosenbluh M., Wilson-Gordon A.D. *J. Opt. Soc. Am. B*, **16**, 1127 (1999).
31. Lamb G.L. Jr. *Phys. Rev. A*, **9**, 422 (1974).
32. Kasapi A., Jain M., Yin G.Y., Harris S.E. *Phys. Rev. Lett.*, **74**, 2447 (1995).